Model many-body Stoner Hamiltonian for binary FeCr alloys

D. Nguyen-Manh and S. L. Dudarev
EURATOM/UKAEA Fusion Association, Culham Science Centre, Abingdon, Oxfordshire OX14 3DB, United Kingdom
(Received 1 December 2008; revised manuscript received 25 August 2009; published 30 September 2009)

We derive a model tight-binding many-body *d*-electron Stoner Hamiltonian for FeCr binary alloys and investigate the sensitivity of its mean-field solutions to the choice of hopping integrals and the Stoner exchange parameters. By applying the local charge-neutrality condition within a self-consistent treatment we show that the negative enthalpy-of-mixing anomaly characterizing the alloy in the low chromium concentration limit is due entirely to the presence of the *on-site* exchange Stoner terms and that the occurrence of this anomaly is not specifically related to the choice of hopping integrals describing conventional chemical bonding between atoms in the alloy. The Bain transformation pathway computed, using the proposed model Hamiltonian, for the $Fe_{15}Cr$ alloy configuration is in excellent agreement with *ab initio* total-energy calculations. Our investigation also shows how the parameters of a tight-binding many-body model Hamiltonian for a magnetic alloy can be derived from the comparison of its mean-field solutions with other, more accurate, mean-field approximations (e.g., density-functional calculations), hence stimulating the development of large-scale computational algorithms for modeling radiation damage effects in magnetic alloys and steels.

DOI: 10.1103/PhysRevB.80.104440 PACS number(s): 75.50.Bb, 71.20.Be, 71.15.Mb

I. INTRODUCTION

Developing predictive models for magnetic ferritic and ferritic-martensitic steels that exhibit higher resistance to irradiation than other steels, and using mathematical modeling as an exploratory tool for investigating possible alternative compositions and microstructures, requires formulating controlled approximations and simplified numerical algorithms for large-scale computer simulations.[1,2] For the case of binary FeCr alloys, which are model materials with properties resembling those of ferritic and ferritic-martensitic steels, density-functional theory (DFT) calculations have recently provided new insights into the origin of the negative enthalpy-of-mixing zero-temperature anomaly characterizing these alloys in the 0–10% Cr concentration range for body-centered-cubic (bcc)-ordered structures[3–8] and for disordered structures investigated in the coherent potential approximations (CPA) (Refs. 9–12). DFT calculations showed that this enthalpy-of-mixing anomaly only occurs for *magnetic* self-consistent solutions, namely, for those where both iron and chromium atoms develop nonzero magnetic moments associated with their *d* shells. Taking into account magnetism also proves necessary for predicting the structure of interstitial and vacancy defects in iron and alloys, and pathways for their thermally activated migration.[5,7,13–15] A recent self-consistent nonorthogonal tight-binding (TB) study of FeCr performed using *spd* basis sets[16] showed that magnetism stabilizes short-range-ordered atomic configurations of FeCr alloys in the low chromium concentration limit.[17,18] However, the above study,[16] involving a significant number of adjustable parameters, leaves open the question about a *minimum parameter set* model capable of describing the unusual properties of FeCr alloys.

In this paper we prove that a *d*-band-only many-body TB model, based on a simple quantum-mechanical model Hamiltonian and including only the *on-site* exchange interactions between electrons, which in the mean-field approximation converges to a model applied earlier to pure iron,[19–21] is capable of reproducing at close to quantitative level of accuracy the negative enthalpy-of-mixing anomaly characterizing FeCr alloys, as well as the complex magnetic configurations of the alloys found earlier in DFT calculations.

The need for developing a methodology for modeling high-temperature properties of iron alloys and steels requires going beyond the zero-Kelvin mean-field approximation. For instance, thermal fluctuations of magnetic moments are responsible for the occurrence of unusual dislocation structures observed in iron and FeCr alloys irradiated at temperatures approaching 500 °C.[22–25] Similarly, magnetic fluctuations and the resulting strong variation in elastic constants as functions of temperature[23,25–27] result in the loss of mechanical strength of ferritic and ferritic-martensitic steels at elevated temperatures.[28,29] Modeling thermal magnetic excitations involves going beyond the mean-field single-particle treatment of electronic structure adopted in recent studies,[16,19] and requires using a full operator expression for the many-body TB Hamiltonian.[27]

A model Hamiltonian describing an isolated lattice site occupied by interacting electrons and linked to the sea of noninteracting electronic states was proposed by Anderson,[30] who followed earlier work by Friedel.[31] Hubbard[32] extended the treatment to the case of a lattice, still treating only the direct on-site Coulomb interaction between electrons for a *nondegenerate*, single-orbital per lattice site, case. Later, this nondegenerate single-orbital-per-site model was applied to the investigation of magnetism in iron.[33] In these studies,[30,32,33] the on-site interaction between electrons was described by the Hubbard *U*-term (note that in Ref. 32 parameter *U* was denoted by *I*). Since the notion of on-site exchange interaction does not arise in the single *s*-orbital-per-site limit, the effects of exchange interaction were not included in the analysis performed in Refs. 30, 32, and 33.

Exchange interactions play a particularly significant part for *d*-electron metals, where the mean-field Stoner model[34] allows the TB approximation to be applied to the investigation of magnetic solutions. This model, which treats the on-

site exchange interactions via the effective spin-dependent on-site energies, can be derived from DFT.[35] For applications going beyond the analysis of zero-temperature ground-state properties,[27] in particular, for those required to model the high-temperature behavior of magnetic alloys, it is necessary to have a mathematical formulation based on a suitable quantum-mechanical operator Hamiltonian, rather than on its mean-field solutions.

In this paper we show how to relate the spin-dependent mean-field Stoner model[19] to a multiband model Stoner operator *Hamiltonian* for interacting d electrons. Bearing in mind the goal of formulating a minimum parameter set model for FeCr magnetic alloys, we focus on a d-band-only Hamiltonian and investigate its mean-field solutions in the local charge-neutrality (LCN) approximation. We find that in order to describe the electronic structure and chemical bonding in FeCr alloys, including the unusual negative heat-of-formation anomaly characterizing the ferromagnetic configuration of the alloys in the 0–10% Cr concentration range, we only need to retain in the second-quantized TB Hamiltonian (in addition to the usual electron-hopping terms and the on-site energies) the on-site exchange terms quadratic in the operator of the local magnetic moment. The interplay between the effects of on-site magnetic exchange and intersite electron hopping results in an unusual self-consistent electronic configuration characterized by the negative heat-of-formation anomaly and exhibiting magnetic correlations found also in density-functional calculations.[3–12] The fact that the addition of purely on-site Stoner operator terms has such a strong effect on the electronic structure and chemical bonding is not surprising and represents a manifestation of a general fact that even a simple nonlinear quantum-mechanical Hamiltonian may have fairly complex many-electron eigenstates.[36] For example, the inclusion of purely on-site terms in the LSDA+U treatment of electron correlations is known to have a significant impact on the electronic structure and chemical bonding in transition-metal and actinide oxides.[37]

The paper is organized as follows. In Sec. II we show how a many-orbital-per-site periodic Anderson Hamiltonian[38–42] can be transformed into a many-body many-orbital-per-site Stoner Hamiltonian for an alloy. To parameterize this Hamiltonian, in Sec. III we investigate its mean-field solutions and compare them with DFT calculations. In this way we are able to select optimal values for the TB hopping integrals, the on-site Stoner parameters, and the average on-site d-electron occupation numbers. We find that all the main features characterizing the alloy, including the anomalous negative enthalpy-of-mixing and the Bain transformation pathways investigated in Sec. IV for a representative low Cr concentration alloy configuration, can be well described by this d-electron-only TB Hamiltonian. Furthermore, we discover that the choice of hopping integrals does not influence the self-consistent solutions as strongly as the presence of the intra-atomic on-site Stoner exchange terms. To illustrate this point, in Sec. V we compare the present d-only orthogonal TB Stoner Hamiltonian model with the nonorthogonal *spd* magnetic TB calculations.[16] Section VI summarizes the main results and concludes the paper.

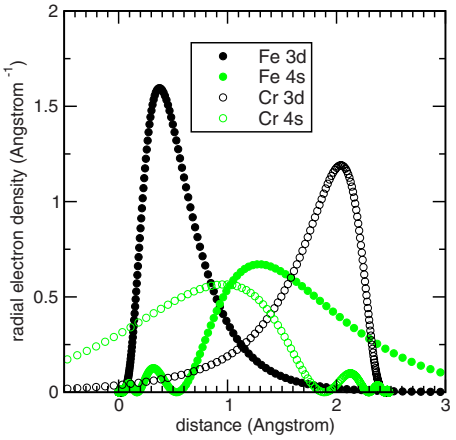

FIG. 1. (Color online) Normalized radial probability densities for the 3d and 4s electronic states evaluated in the local-density approximation for a pair of isolated iron and chromium atoms. The figure shows overlap between atomic orbitals centered on an iron atom (left) and a chromium atom (right). The distance between the atoms in this figure is taken to be the same as the distance between the nearest-neighbor lattice sites in a bcc FeCr alloy.

II. ANDERSON AND THE STONER HAMILTONIANS FOR IRON-CHROMIUM ALLOYS

Binary iron-chromium alloys are unique in the sense that both iron and chromium have bcc low-temperature crystal structures with lattice parameters that differ by less than half a percent. This results in an almost distortion-free crystal structure of the alloy where Fe and Cr atoms occupy nearly ideal bcc lattice sites. In the absence of elastic distortions associated with the atomic size mismatch, the site-occupation probabilities and short-range-order correlation functions are determined by interactions that are much weaker than elastic forces that drive microstructural evolution in many other alloys.[43,44]

To derive a model Hamiltonian for a binary FeCr alloy, we start from the atomic limit. Figure 1 shows the radial electron densities calculated using full-potential linear muffin-tin orbital (FP-LMTO) code[45] within the local-density approximation (LDA) for the 4s and 3d orbitals of iron atoms (left) and chromium atoms (right), plotted as a function of radial coordinates for each atom. The distance between the atoms equals the distance between the nearest-neighbor lattice sites in a typical bcc FeCr alloy. Figure 1 shows that the 4s orbitals are very extended in space whereas the overlap between the 3d orbitals is small, justifying the use of an orthogonal TB model for 3d electrons.[46]

A model Hamiltonian, which describes electron hopping, as well as on-site electron-electron interactions for the case of a fivefold-degenerate 3d band, was proposed by Anderson.[38,39] This Hamiltonian has a general form[40–42]

$$\hat{H} = \sum_{i,j,\ i\neq j} \sum_{m,m',\sigma} t_{im,jm'} \hat{c}^{\dagger}_{im\sigma} \hat{c}_{jm'\sigma} + \sum_{i,m,\sigma} \epsilon_i \hat{c}^{\dagger}_{im\sigma} \hat{c}_{im\sigma} + \sum_i \left[\frac{\bar{U}_i}{2} \sum_{m,m',\sigma} \hat{n}_{im,\sigma} \hat{n}_{im',-\sigma} + \frac{\bar{U}_i - \bar{J}_i}{2} \sum_{m,m',\sigma} \hat{n}_{im,\sigma} \hat{n}_{im',\sigma} (1 - \delta_{mm'}) \right], \quad (1)$$

where the t terms describe quantum hopping between ions (lattice sites) i and j, $\hat{c}^{\dagger}_{im\sigma}$ and $\hat{c}_{jm'\sigma}$ are the second-quantized creation and annihilation operators, ϵ_i are the single-particle on-site energies, and $\hat{n}_{im,\sigma}=\hat{c}^{\dagger}_{im\sigma}\hat{c}_{im\sigma}$ is the operator for the number of electrons occupying orbital m on site i. Parameter $\bar{U}_i$ describes the Coulomb energy of repulsion between a pair of electrons occupying the same lattice site with antiparallel spin whereas $\bar{J}_i$ described the reduction in the strength of Coulomb repulsion for the case where the spins of electrons are parallel. Parameters $\bar{U}_i$ and $\bar{J}_i$ are related to Slater's integrals.[37,47] By assuming their independence of d-orbital indexes m and m', we neglect the crystal-field effects.[48,49] Finally, in Eq. (1) the $1-\delta_{mm'}$ factor accounts for the Pauli exclusion principle.

Noting that $\hat{n}^2_{im,\sigma}=\hat{n}_{im,\sigma}$, we transform the last term in Eq. (1) as

$$\frac{\bar{U}_i-\bar{J}_i}{2}\sum_{m,m',\sigma}\hat{n}_{im,\sigma}\hat{n}_{im',\sigma}(1-\delta_{mm'}) = \frac{\bar{U}_i-\bar{J}_i}{2}\sum_{\sigma}(\hat{N}_{i,\sigma}\hat{N}_{i,\sigma}-\hat{N}_{i,\sigma}), \tag{2}$$

where $\hat{N}_{i,\sigma}=\Sigma_m\hat{n}_{im,\sigma}$ is the operator for the total number of electrons with spin σ occupying site i. Similarly, the first term in square brackets in Eq. (1) has the form $(\bar{U}_i/2)\Sigma_\sigma\hat{N}_{i,\sigma}\hat{N}_{i,-\sigma}$. Hamiltonian (1) can now be written in a compact form, which is still fully equivalent to Eq. (1), as

$$\hat{H}=\sum_{i,j,\ i\neq j}\sum_{m,m',\sigma}t_{im,jm'}\hat{c}^{\dagger}_{im\sigma}\hat{c}_{jm'\sigma}+\sum_{i,m,\sigma}\epsilon_i\hat{c}^{\dagger}_{im\sigma}\hat{c}_{im\sigma} +\sum_{i,\sigma}\left[\frac{\bar{U}_i}{2}\hat{N}_{i,\sigma}\hat{N}_{i,-\sigma}+\frac{\bar{U}_i-\bar{J}_i}{2}(\hat{N}^2_{i,\sigma}-\hat{N}_{i,\sigma})\right]. \tag{3}$$

By rearranging terms in square brackets in Eq. (3), we now prove that there is a connection between this Hamiltonian and the Stoner Hamiltonian postulated by Hasegawa *et al.*[27]

Introducing operators $\hat{N}_i=\hat{N}_{i\uparrow}+\hat{N}_{i\downarrow}$ and $\hat{M}_i=\hat{N}_{i\uparrow}-\hat{N}_{i\downarrow}$, we transform Eq. (3) as

$$\hat{H}=\sum_{i,j,\ i\neq j}\sum_{m,m',\sigma}t_{im,jm'}\hat{c}^{\dagger}_{im\sigma}\hat{c}_{jm'\sigma}+\sum_i\epsilon_i\hat{N}_i +\sum_i\left[\frac{\bar{U}_i}{2}(\hat{N}^2_i-\hat{N}_i)-\frac{\bar{J}_i}{4}(\hat{N}^2_i-2\hat{N}_i)-\frac{\bar{J}_i}{4}\hat{M}^2_i\right]. \tag{4}$$

The first term in square brackets in the above equation is a quantum-mechanical analog of the classical expression for the energy of Coulomb interaction between N_i electrons occupying the same lattice site. The second term, which is also a function of $\hat{N}_i$, is a small correction to the first term and, if necessary, can be neglected within the framework of the present model. The last term in square brackets in Eq. (4) is the only term in the entire Hamiltonian that depends on the local magnetic moment $\hat{M}_i$. Neglecting fluctuations of the total number of electrons occupying a lattice site (in this way we effectively include the $\hat{N}_i$-dependent terms in the definition of the on-site energies $\tilde{\epsilon}_i$), we arrive at the model Stoner Hamiltonian[27]

$$\hat{H}=\sum_{i,j,\ i\neq j}\sum_{m,m',\sigma}t_{im,jm'}\hat{c}^{\dagger}_{im\sigma}\hat{c}_{jm'\sigma}+\sum_i\tilde{\epsilon}_i\hat{N}_i-\frac{1}{4}\sum_i I_i\hat{M}^2_i. \tag{5}$$

Here we note that the intra-atom exchange parameters $\bar{J}_i$ of the multiorbital periodic Anderson Hamiltonian (1) that we used as a starting point for the derivation, are exactly equal to the Stoner parameters I_i, see Ref. 42.

To find the mean-field solutions for Hamiltonian (4), we follow Anderson[30] and define the one-particle Green's function $G^{\sigma}_{im;jm'}(\epsilon)$. The equations of motion for this Green's function have the form[30]

$$(\epsilon-\epsilon^{\sigma}_i)G^{\sigma}_{im;jm'}(\epsilon)-\sum_{k\neq i,m''}t_{im,km''}G^{\sigma}_{km'';jm'}(\epsilon)=\delta_{ij}\delta_{mm'}, \tag{6}$$

where

$$\epsilon^{\sigma}_i=\epsilon_i-\frac{\bar{U}_i-\bar{J}_i}{2}+\left[\bar{U}_i-\frac{\bar{J}_i}{2}\right]\langle N_i\rangle-\frac{\bar{J}_i}{2}\sigma\langle M_i\rangle \tag{7}$$

and where $\langle N_i\rangle$ is the expectation value for the operator of the total number of electrons occupying site i. Similarly, $\langle M_i\rangle$ is the expectation value for the operator of the total magnetic moment associated with site i.

The fact that the effective on-site energies ϵ^{σ}_i in Eq. (6) depend on the projection of spin σ and that this dependence has the form $\pm\bar{J}_i\langle M_i\rangle/2$, is a well-known feature of the *mean-field* TB Stoner model.[16,19] For example, Eq. (6) of Ref. 19

$$\epsilon^{\sigma}_i=\epsilon_i-\frac{I}{2}\sigma\langle M_i\rangle, \tag{8}$$

is identical to Eq. (7), subject to the charge-neutrality condition and subject to the treatment of on-site energies as occupation number-dependent quantities. We reiterate here that the TB Stoner model [Eqs. (7) and (8)], investigated earlier in Refs. 16 and 19, is a single-particle mean-field approximation, i.e., an approximation that can be derived from the full operator Stoner Hamiltonian (5).

In the (physically unreasonable for d electrons) limit $\bar{U}_i=\bar{J}_i$, where the Anderson Hamiltonian (1) coincides with the Hubbard Hamiltonian,[50] from Eq. (7) we find the effective on-site energies

$$\epsilon^{\sigma}_i=\epsilon_i+\bar{U}_i\langle N_{i,-\sigma}\rangle. \tag{9}$$

This equation is identical to Eq. (15) of Ref. 30 and is only valid in the single s-orbital-per-site limit. For a general case, where $\bar{U}_i\neq\bar{J}_i$, from Eq. (7) we find an expression for the on-site energies

$$\epsilon_i^\sigma = \epsilon_i - \frac{\bar{U}_i - \bar{J}_i}{2} + \left[\bar{U}_i - \frac{\bar{J}_i}{2}\right]\langle N_i\rangle - \frac{\bar{J}_i}{2}\sigma\langle M_i\rangle$$

$$= \epsilon_i - \frac{\bar{U}_i - \bar{J}_i}{2} + \bar{U}_i\langle N_i\rangle - \frac{\bar{J}_i}{2}[\langle N_i\rangle + \sigma\langle M_i\rangle]$$

$$= \epsilon_i - \frac{\bar{U}_i - \bar{J}_i}{2} + \bar{U}_i\langle N_i\rangle - \bar{J}_i\langle N_{i,\sigma}\rangle, \quad (10)$$

in deriving which we employed the condition $\langle N_i\rangle + \sigma\langle M_i\rangle = 2\langle N_{i,\sigma}\rangle$.

Equation (10) shows that there is a fundamental link between the Anderson [Eq. (9)] (Ref. 30) and the Stoner [Eq. (8)] (Refs. 19 and 27) models. According to the argument given above, the two models represent limiting cases for the same general Hamiltonian (1).

In a metal, the nearly perfect screening results in ions being effectively locally charge neutral.[46] Hence, in what follows the expectation values of $\langle N_i\rangle$ can be taken as constants. In Eq. (10) there is only one term $\bar{J}_i\langle N_{i,\sigma}\rangle$ that depends on the projection of spin. This shows that in a transition-metal alloy it is the intra-atomic on-site Stoner exchange, described by parameters $\bar{J}_i \equiv I_i$, and not the Hubbard on-site Coulomb interaction, described by the $\bar{U}_i$ terms, that determine the magnetic configuration of the alloy.

III. MEAN-FIELD SOLUTIONS FOR THE STONER HAMILTONIAN

In a numerical implementation of the TB model for FeCr alloys the self-consistent Eq. (6) is complemented by the condition defining the total number of electrons on each lattice site

$$\langle N_{i,\sigma}\rangle = -\frac{1}{\pi}\int_{-\infty}^{\epsilon_F}\sum_m \Im G^\sigma_{im;im}(\epsilon + i0)d\epsilon = \sum_m \rho^\sigma_{im,im}, \quad (11)$$

where ϵ_F is the Fermi energy and $\rho^\sigma_{im,im}$ is a diagonal element of the density matrix. The on-site magnetic moment is given by $\langle M_i\rangle = \Sigma_m[\rho^\uparrow_{im,im} - \rho^\downarrow_{im,im}]$.

In the preceding section we showed that the Stoner Hamiltonian (5), the mean-field solutions of which are uniquely and fully defined by the spin-dependent on-site energies [Eq. (8)], is related to the mean-field TB bond (TBB) Stoner model developed earlier for magnetic bcc iron.[19–21]

In the original TBB model,[51] as well as in its mean-field generalization to magnetic transition metals,[19] the crystal-field effects, giving rise to the multiplet splitting of the on-site energies for the initially degenerate d-orbital states,[52] were neglected. This approximation is consistent with the many-body Hamiltonian (1) where we neglected the dependence of the Hubbard $\bar{U}$ and exchange $\bar{J}$ parameters on the orbital indexes m and m'.

We now apply the model to the treatment of a magnetic binary alloy to see if the model, parameterized in the simplest possible way, is able to describe the anomalous variation in the enthalpy-of-mixing treated as a function of chromium concentration.[3–5,9,10] We also investigate what terms in Hamiltonian (5) are responsible for the negative enthalpy-of-mixing of the alloy occurring in the low chromium concentration limit.

The electronic part of the total energy of the alloy in the TBB model is given by the expectation value of the Stoner Hamiltonian (5), namely,[19]

$$E_{\mathrm{TBB}} = \sum_{i,j,\ i\neq j}\sum_{m,m',\sigma}\rho^\sigma_{im;jm'}t_{jm',im} - \frac{1}{4}\sum_i I_i\langle M_i\rangle^2, \quad (12)$$

where $\rho^\sigma_{im;jm'}$ are the site off-diagonal elements of the density matrix. In Eq. (12) the contribution from the on-site energy terms is absent due to the assumed validity of the LCN condition that keeps constant the total electron site-occupation numbers $\langle N_i\rangle$.

The TBB model [Eq. (12)] for a FeCr binary alloy on a bcc lattice was implemented within the OXON code.[53] Earlier studies of nonmagnetic transition-metal alloys showed that the appropriate choice of numerical values for hopping integrals $t_{jm',im}$ was essential for ensuring the physically sensible behavior of the model.[54] Since we are interested in developing the simplest possible model for magnetic FeCr alloys, we adopt a more restricted subset of electronic states than that used by Paxton *et al.*,[16] where a full set of s, p, and d orbitals was included in the treatment. We consider only the d-d hopping integrals for $3d$ electrons that dominate bonding in transition metals.[46] A detailed comparison of the present model with the *spd* model of Ref. 16 is given in Sec. V.

We carry out two case studies, aimed at elucidating the role played by the two physically distinct contributions to Hamiltonian (5), namely, the contributions associated with the difference between the hopping integrals involving the iron-iron, iron-chromium, and chromium-chromium pairs of atoms, and the contributions from the on-site Stoner terms. Both contributions can, in principle, affect the electronic structure and interatomic bonding in the alloy.

In case study I, we take the $3d$ hopping integrals for the Fe-Fe, Cr-Cr, and FeCr bonds as identical to those of pure iron. This assumption corresponds to the so-called rigid-band approximation. The values of TB parameters for this case are taken from our previous study,[19] where the first nearest-neighbor (1NN) integrals $(dd\sigma, dd\pi, dd\delta)$ are equal to $(-0.6877, 0.4196, -0.0392)$ eV. These numerical values were derived from the DFT-based third-generation orthogonal TB-LMTO analysis.[55]

In case study II, the Cr-Cr hopping integrals were derived from a similar TB-LMTO electronic-structure calculation performed for pure bcc Cr. Here the 1NN hopping integrals $(dd\sigma, dd\pi, dd\delta)$ are equal to $(-0.9222, 0.5441, -0.0427)$ eV, respectively. In case study II the mixed FeCr hopping integrals are taken as the geometric mean between the Fe-Fe and Cr-Cr values, e.g., $|dd\pi(\mathrm{FeCr})| = \sqrt{|dd\pi(\mathrm{FeFe})| \times |dd\pi(\mathrm{CrCr})|}$. The sign for a "mixed" hopping integral is the same as for a pure metal. The magnitude of Cr-Cr hopping integrals derived from TB-LMTO calculations is larger than that for bcc Fe, in agreement with the curves shown in Fig. 1, where the degree of overlap between

the 3*d* orbitals of Cr atoms is greater than that for the 3*d* orbitals of Fe atoms.

The enthalpy-of-mixing for binary FeCr alloy, where ferromagnetic bcc Fe and antiferromagnetic bcc Cr serve as two reference points, was evaluated for both case studies, and the predicted values were compared with results of DFT calculations performed for various alloy configurations.[20,21,56] In both cases, the average number of electrons occupying a Fe lattice site $N_d(\mathrm{Fe})=6.8$, and the on-site Stoner parameter $I_d(\mathrm{Fe})=0.77$ eV for an iron ion, were assumed to be the same as in our earlier study.[19] Results derived from magnetic and nonmagnetic calculations are shown in Fig. 2 for the rigid-band approximation (case study I), where the hopping integrals for the Fe-Fe, Cr-Cr, and FeCr bonds are assumed to be identical, and for a more realistic case (case study II), where the hopping integrals are taken as site-dependent quantities. The choice of hopping integrals influences the choice of the total number of electrons on the Cr sites and the choice of the Stoner parameter for the Cr atoms $I_d(\mathrm{Cr})$. For case study I the total number of electrons per chromium site is $N_d(\mathrm{Cr})=5.7$ and the Stoner parameter is $I_d(\mathrm{Cr})=0.38$ eV whereas for case study II, where the choice of Cr-Cr hopping integrals is consistent with the TB-LMTO electronic structure of pure chromium, the optimum choice of parameters is $N_d(\mathrm{Cr})=5.4$ and $I_d(\mathrm{Cr})=0.54$ eV. The values of $I_d(\mathrm{Cr})$ and $N_d(\mathrm{Cr})$ are optimized to reproduce the very small positive-energy difference between the nonmagnetic (NM) and antiferromagnetic (AFM) phases of bcc chromium (9 meV/atom, as found in DFT calculations[57]).

Our previous investigation of the TBB Stoner model for iron has already shown good qualitative agreement with DFT calculations for the energy differences between the FM, AFM, and NM phases for bcc, fcc, and hcp crystal structures.[19] The fact that the Stoner parameter found in our current study for a Cr atom $I_d(\mathrm{Cr})$ is smaller than that for a Fe atom is in broad agreement not only with the *spd* investigation of FeCr clusters[58] but also with the trend found in DFT calculations for the 3*d* transition-metal series.[59]

The calculated values for the enthalpy-of-mixing shown in Fig. 2 were determined using both spin-polarized (magnetic) and non-spin-polarized (nonmagnetic) calculations for alloy configurations $Fe_{15}Cr$ (15sc222), $Fe_{25}Cr_2$, Fe_7Cr (14sc222), Fe_3Cr (DO_3 and tP8-L62–1), FeCr (B2 and tP8-L44–1), $FeCr_3$ (DO_3 and tP8-L62–1), and $FeCr_{15}$ (15sc222) discussed in detail in Refs. 5 and 6. In this notation, 15sc222 means that the corresponding alloy configuration is constructed from a $2\times2\times2$ supercell of bcc lattice containing 15 Fe atoms. Similarly, in the case of 14sc222 configuration there are 14 Fe atoms and two Cr atoms occupying sites (0,1/2,1/2) and (1/2,0,0). The structure of $Fe_{25}Cr_2$ is derived from a $3\times3\times3$ supercell, where positions of Cr atoms are (1/6,1/6,1/6), (1/6,5/6,5/6), (5/6,1/6,5/6), and (5/6,5/6,1/6) [see also Fig. 3b of Ref. 6]. Finally, tP8-L62–1 denotes a tetragonal structure with four bcc unit cell along the [001] direction in which six layers are formed by type A atoms and the other two layers by type B atoms. Similarly, tP8-L44–1 denotes a tetragonal structure with four type A and four type B atomic layers. These structures represent segregated layered configurations and they have the lowest enthalpy of mixing for a given Cr concentration, as found in our earlier DFT study.[5] To complete the analysis, we have also investigated the enthalpy-of-mixing for the σ phase, for which we assumed the Fe_3Cr_2 alloy composition, corresponding to the fully occupied Fe(2a)Cr(4f)Cr(8i)Fe(8i)Fe(8j) configuration [in Wyckoff's multiplicity index notation for the tetragonal tP30 ($P4_2/mmm$) symmetry of the structure]. This configuration was investigated by Korzhavyi *et al.*[60] within the disordered local-moment (DLM) approximation. The distribution of magnetic moments found in DFT and Stoner Hamiltonian-model calculations for these five symmetry sites in the σ-phase crystal structure was discussed in Ref. 56.

Figure 2 shows that for cases I and II the Stoner 3*d* model reproduces fairly accurately the crossover between the regions of negative and positive enthalpies of mixing. It also shows that there is very good agreement between the enthalpies of mixing found for various magnetic and nonmagnetic ordered structures, including the σ phase, for the entire range of chromium concentrations between 0 and 100%. For the $Fe_{15}Cr$ structure the enthalpies of mixing calculated for the ferromagnetic and nonmagnetic configurations of the alloy are −0.0069 and 0.4304 eV (−0.0079 and 0.4383 eV) for case studies I(II), respectively. These 3*d* Stoner model values agree very well with the corresponding DFT values of −0.0065 and 0.4317 eV.

Figure 2 suggests that the overall accuracy of the parameter set used for case study II is higher than that of the parameter set used in case study I. This is not surprising given the more realistic description of the band structure of the alloy achieved in case study II due to a better choice of hopping integrals. The agreement between case study II and DFT calculations is particularly good for the lowest-energy alloy configurations, for example, the layered structures tP8-L62 and tP8-L44, where the enthalpies of formation are within the ±0.025 eV (±300 K) per atom range. This analysis shows that while the origin of the "anomalous" negative enthalpy-of-mixing of the alloy in the ~10% Cr concentration range is associated with the presence of the Stoner on-site exchange terms $-I_i\hat{M}_i/4$ in Hamiltonian (5), giving rise to symmetry-broken magnetic solutions, a quantitative treatment of enthalpies of mixing for the alloy in the entire chromium concentration range also requires taking into account the difference between the 3*d* orbitals of iron and chromium ions.

To extend this analysis beyond the total-energy calculations we compared the magnetic structures found in case studies I and II for the B2 phase with those predicted by spin-polarized DFT calculations. The energy difference between the nonmagnetic and magnetic configurations for the B2 phase is 0.1358 eV (0.0844 eV) for case studies I(II), compared to the DFT energy difference of 0.1082 eV.

For $Fe_{15}Cr$ phase, the electronic structure and stability were investigated earlier using both the DFT-based,[7,56] and TB *spd*-model[16] approaches. In $Fe_{15}Cr$ structure each chromium atom is surrounded by iron atoms occupying the first, second, third, fourth, and the fifth coordination shells. DFT calculations show that in the symmetry-broken lowest-energy magnetic state the magnetic moments of Cr ions are ordered antiferromagnetically with respect to the ferromag-

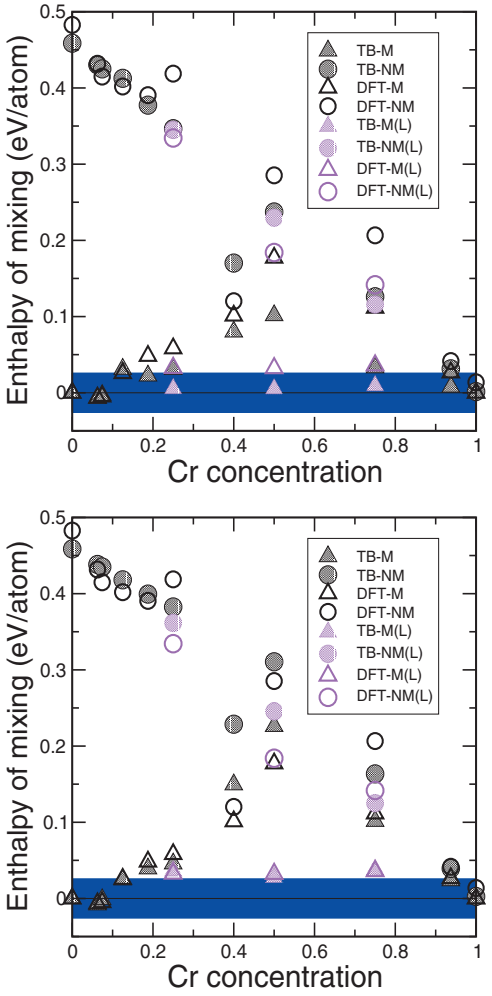

FIG. 2. (Color) The enthalpy-of-mixing for binary FeCr alloys evaluated using the TB mean-field solutions of Hamiltonian (5), shown together with the corresponding values found by DFT calculations for magnetic and nonmagnetic (NM) configurations. The top graph shows results found for case study I, where all the hopping integrals were assumed to be the same as in pure iron and where only the Stoner parameters for Fe and Cr sites were adjusted. The bottom graph illustrates case study II, where hopping integrals for Cr atoms were derived from the band structure of pure chromium, as described in the text. The subset of layered structures tP8-L62–1 and tP8-L44–1 is denoted by L. The colored band at the bottom of each figure gives the scale of thermal-energy fluctuations (per atom) at room temperature.

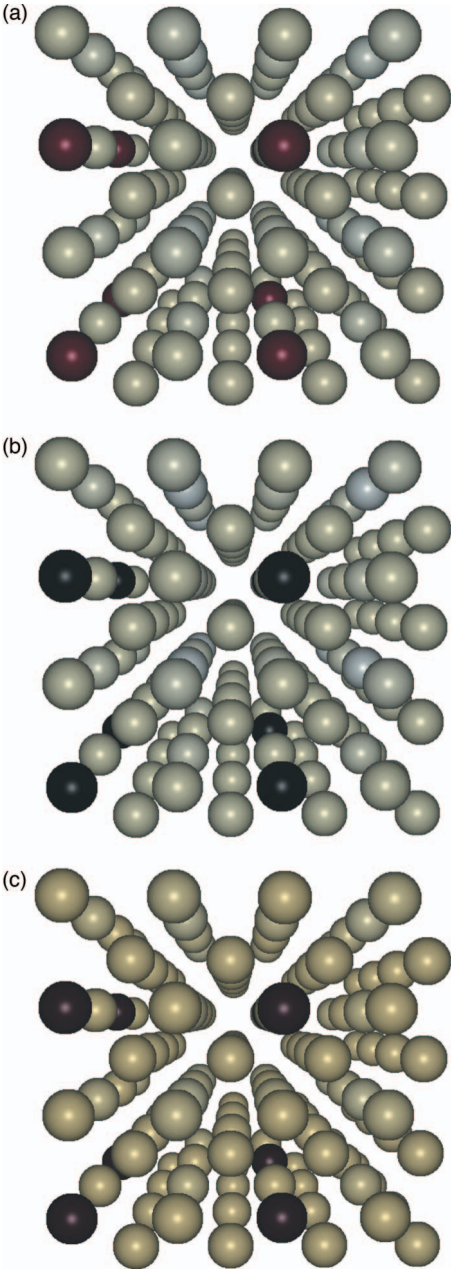

FIG. 3. (Color) The magnetic configurations of bcc-like $Fe_{15}Cr$ alloy found using the mean-field solutions of Hamiltonian (5) and density-functional theory calculations. (a) case study I, (b) case study II, and (c) DFT. The color of atoms in the structures represents the magnitude and the direction (+ up and − down) of magnetic moments: +3 μ_B is pure gray and −2 μ_B is pure black.

netically ordered moments of iron atoms. Figure 3 shows, in pictorial form, the magnetic-moment configurations found using Hamiltonian (5) for case studies I and II, and the one found using DFT calculations. The color scheme used in the figure is the same for all the three cases. We see that in all the cases shown in the figure the magnetic moments of Cr atoms are ordered antiferromagnetically relative to the ferromagnetically ordered moments on Fe sites. The magnetic moment on Cr sites is -1.3 μ_B for model I and -2.2 μ_B for model II, compared to the DFT value of -1.7 μ_B. Given that the magnetic moment of pure bcc Fe is overestimated by $\sim 18\%$ within the TB model[19] [for pure iron the mean-field treatment of Hamiltonian (5) gives $M \approx 2.6$ μ_B compared to the DFT value of $M \approx 2.2$ μ_B], we see that a similar scaling factor applies to the chromium magnetic moment predicted by model II within the $Fe_{15}Cr$ phase. This shows that model II provides a good match to DFT results not only for the negative enthalpies of mixing for the various alloy configurations corresponding to low Cr concentrations but also for the predicted low-temperature magnetic structures.

In the next section we apply the model developed above to the treatment of the bcc-fcc transformation pathway for $Fe_{15}Cr$ alloy. Investigating this pathway is of interest in connection with the occurrence of the so-called γ loop in the

high-temperature part of the FeCr phase diagram.[61,62] It is worth emphasizing again here that the experimental FeCr phase diagram[62] is only available for the range of temperatures above approximately 400 °C (673 K), equivalent to the energy of 58 meV per atom, which in turn is located well outside the ±25 meV/atom range shown in Fig. 2. We believe that thermal energy fluctuations on this 25 meV/atom scale are the reason why so far the ordered compound $Fe_{15}Cr$ predicted both by DFT calculations[5,8] and by the present Stoner Hamiltonian model, and characterized by the relatively small negative enthalpy of mixing (less than −10 meV/atom), has not been observed experimentally.

IV. BAIN TRANSFORMATION OF $Fe_{15}Cr$ ALLOY

Changes in microstructure associated with the (bcc) α to (fcc) γ phase transformation in iron, iron-based alloys, and steels are among the most significant factors affecting mechanical and engineering properties of these materials.[61] For example, the strong elastic anisotropy of iron that develops at elevated temperatures, approaching the temperature of the α-γ phase transition, affects the self-energies of dislocations in the material[23,25] as well as the strength of interaction between dislocations,[28,29] giving rise to profound changes in mechanical properties of ferritic steels and iron-based alloys at elevated temperatures. The experimental phase diagram of FeCr binary alloys[62] shows that the high-temperature γ phase spans the low Cr concentration range (0–11%), approximately matching the interval of chromium concentrations where the zero-temperature enthalpy-of-mixing of the alloy is negative. The $Fe_{15}Cr$ alloy composition is of particular interest here since independent DFT calculations predict the $Fe_{15}Cr$ ordered compound as the most stable configuration for various cubic phases.[5,8]

The difference between the energies of these phases is small, enabling us to focus on how the energy of cubic $Fe_{15}Cr$ structure with 16 atoms per unit cell varies along the bcc-like to fcc-like Bain transformation pathway. The curve showing how the energy per atom in the alloy varies as the crystal lattice transforms along the Bain pathway[63] was evaluated using the two numerical parameterizations for the Stoner model described above. The Hamiltonian hopping matrix elements $t_{im,jm'}$ were parameterized as functions of the bond length R_{ij} as power-law functions

$$t(R) = t(R_0)(R_0/R)^n, \tag{13}$$

where R_0 is the nearest-neighbor bond length for the bcc phase and the exponents n for the $dd\sigma$, $dd\pi$, and $dd\delta$ bond integrals are 4.5, 4.0, and 4.0, respectively, as in the case of ferromagnetic iron.[19] The Bain transformation analysis was also performed using DFT calculations. Figure 4 shows how the energy per atom varies as a function of the tetragonal c/a ratio at the fixed equilibrium volume of bcc-like $Fe_{15}Cr$ structure derived from DFT. The minimum of the curve is at $c/a=1.0$ for case studies I and II, in full agreement with DFT. At $c/a=\sqrt{2}$ the $Fe_{15}Cr$ alloy adopts an fcc-like structure and Fig. 4 shows that the fcc-bcc energy differences predicted by the Stoner models I and II are both in good agreement with DFT calculations. The average magnetic moments

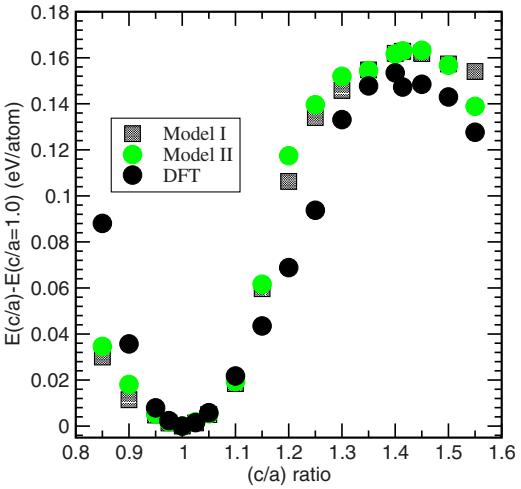

FIG. 4. (Color online) Energy curves corresponding to the Bain transformation pathway for the bcc-like $Fe_{15}Cr$ alloy structure shown in Fig. 3. The points represent energies of deformed structures evaluated using the mean-field solutions of Hamiltonian (5) for the choice of parameters corresponding to case studies I and II, and energies derived from DFT calculations.

found for the fcc-like phases are 2.46 μ_B, 2.51 μ_B, and 2.32 μ_B for models I, II, and DFT, respectively. Comparing this with spin-polarized configurations for fcc iron investigated earlier by Herper *et al.*,[64] we see that it is the high-spin configuration that represents the ground state of the electronic subsystem in the fcc-like $Fe_{15}Cr$ structure.

The elastic constants for bcc-like $Fe_{15}Cr$ alloy structure evaluated using DFT calculations[65] are $(C_{11}, C_{12}, C_{44}) = (243, 132, 101)$ GPa for the spin-polarized state and $(C_{11}, C_{12}, C_{44}) = (-2, 252, 122)$ GPa for the nonspin-polarized (nonmagnetic) state. These sets of values show that $C' = (C_{11} - C_{12})/2$ is negative for the nonspin-polarized configuration and is positive for the spin-polarized state, confirming that magnetic symmetry breaking due to the Stoner terms in Hamiltonian (5) stabilizes the bcc-like phase of FeCr alloys in the low Cr concentration limit.

V. FROM THE STONER HAMILTONIAN TO LARGE-SCALE SIMULATIONS

The analysis of phase stability and magnetic configurations for FeCr binary alloys performed above shows that the treatment based on the mean-field solutions for the TB $3d$-only Stoner Hamiltonian (5) agrees well with DFT calculations. In this section, we discuss implications of these findings for the development of large-scale atomistic models for irradiated magnetic FeCr alloys. The two issues central to this development are (i) the construction of magnetic interatomic potentials for molecular-dynamic simulations and (ii) the development of a quantitative treatment of magnetic fluctuations at elevated temperatures. Addressing both issues requires a suitable Stoner Hamiltonian (5).

Our model TB Stoner Hamiltonian involves only d orbitals, which is an approximation that one has to justify by comparing the solutions found for this Hamiltonian with the

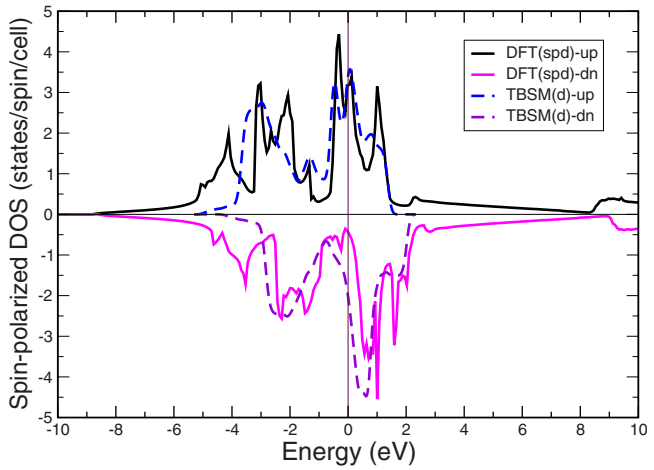

FIG. 5. (Color online) The spin-polarized densities of states calculated for $Fe_{15}Cr$ in bcc-like crystal structure within the present TB *d*-orbital-only Stoner model and those evaluated using self-consistent *spd* DFT LMTO method.

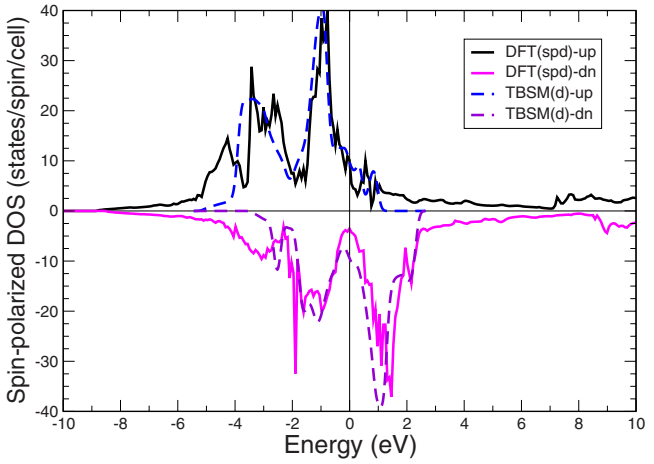

FIG. 6. (Color online) The spin-polarized densities of states calculated for the B2 crystal structure within the present TB *d*-orbital-only Stoner model and those evaluated using self-consistent *spd* DFT LMTO method.

more accurate *ab initio* calculations, as well as with the *spd* TB model calculations performed for the same system. Figure 5 shows the total spin-polarized electronic densities of states (DOS) for the bcc-like $Fe_{15}Cr$ structure calculated using mean-field solutions for Hamiltonian (5) compared with fully self-consistent DFT calculations performed using the minimal *spd* basis set implemented within LMTO method in the atomic sphere approximation (ASA).[66] We see that the DOS predicted by the TB Stoner model agrees well with the spin-up and spin-down *d*-electron-only DOS predicted by the LMTO-ASA calculations. Similarly good agreement was found earlier for the nonmagnetic DOS evaluated for bcc Fe using TB and FP-LMTO calculations.[67]

The *d*-orbital-only model introduced above involves two significant approximations. The first one, illustrated in Fig. 5, involves neglecting the *s*-*d* hybridization effects that give rise to broadening of the *s*-*d* band in comparison with the *d*-band-only limit. The earlier seminal work by Heine[68] showed that the treatment of *sp*-*d* hybridization in transition metals can be implemented through the use of a hybrid representation involving the nearly-free-electron description of *sp* electrons and the TB representation for the *d* electrons. Although, in principle, it is possible to treat the *sp* electrons within the TB scheme, this proves to be computationally expensive due to the long-range nature and the strongly overlapping character of the *s* and *p* orbitals.[69,70] Because of this fact, although a self-consistent *spd* TB magnetic model[16] agrees better with the spin-polarized DFT DOS calculations (see, for example, Fig. 12 of Ref. 16), it is difficult to extend it to large-scale calculations. For example, in the *spd* TB treatment of the $Fe_{15}Cr$ structure the local environment of each Cr atom must include at least 58 neighboring atoms[5,7,71] to describe the Cr-Cr interactions.

The short-range *d*-band model for cohesion of transition metals proposed by Friedel[72] and Pettifor,[46] and implemented in our study, is far simpler and is easier to link with, say, molecular-dynamic simulations. Furthermore, in the *d*-electron-only TB model the *sp*-*d* overlap repulsion effects can be incorporated into an empirical pairwise repulsive potential[21] since it is reasonable to assume that no *sp*-*d* charge transfer occurs in a metal. Recent TB studies of local magnetic configurations around self-interstitial atom point defects[19] and screw dislocations[21] confirmed that the TB *d*-band models provide a good match to DFT calculations for point and extended defects in magnetic iron.

In our TB treatment of on-site exchange we also neglect the crystal-field effects. Figure 5 shows that the fine structure of the DOS spectra associated with the crystal-field splitting of the t_{2g} and e_g manifolds found in DFT calculations is well described by the *spd* TB model.[16] However, this required including a large number of parameters in the model at the expense of its tractability and in fact the inclusion of the crystal-field effects is not fully consistent with the assumption, also adopted in Ref. 16, that the Hubbard $\bar{U}$ and the exchange $\bar{J}$ parameters were treated as *d*-orbital-independent quantities.

Figure 6 shows the spin-polarized DOS evaluated for the B2 phase using the present TB Stoner model and the LMTO-ASA method. Similarly to the case of the $Fe_{15}Cr$ alloy configuration, the shape of the DOS curves is described qualitatively well in comparison with DFT and TB *spd* results illustrated, for example, in Fig. 10 of Ref. 16. The local magnetic moments on Fe and Cr sites are 1.81 μ_B and 0.22 μ_B, respectively, compared with 1.14 μ_B and 0.71 μ_B found using the *spd* TB model,[16] 1.46 μ_B and 0.34 μ_B found in LDA FP-LMTO calculations[16] and 1.71 μ_B and 0.17 μ_B predicted by projector-augmented wave (PAW) generalized gradient approximation-Perdew-Burke-Ernzerhof (GGA-PBE) VASP calculations.[65] Taking into account the approximate nature of the Stoner Hamiltonian model (5), it is encouraging to see that our results are in good agreement with DFT calculations.

Finally, why is it necessary to look for a model Stoner Hamiltonian? First of all, the availability of a many-body Hamiltonian with well-defined hopping integrals and exchange parameters provides a starting point for the treatment of finite-temperature excitations and high-temperature prop-

erties of the alloy.[27] Furthermore, the development of interatomic potentials for molecular dynamics and spin-lattice dynamics requires making further approximations in the treatment of the electronic degrees of freedom, and this can only be achieved by relating certain terms in the Hamiltonian to properties of perfect lattices, alloy configurations, and defects simulated using large-scale algorithms.[67,73] This is also important for the development of large-scale Monte Carlo simulation methods for FeCr alloys, as illustrated by the applications of magnetic cluster expansion, where the interaction parameters derived from a spin-polarized DFT database for FeCr alloys were used as input for a treatment of compositional and high-temperature magnetic orientational disorder in a magnetic alloy.[74]

VI. CONCLUSIONS

The problem of phase stability of iron-chromium alloys has so far been mainly investigated using variational density-functional theory calculations, with finite-temperature analysis focused on mapping the ground-state configurations onto classical spin-lattice models. In this work we show how density-functional theory calculations can be mapped onto a model many-body *d*-electron tight-binding Stoner Hamiltonian for FeCr alloys.

We find that the mean-field solutions generated using a 3*d* TB many-body model Stoner Hamiltonian (5) accurately match the ground-state energies and magnetic configurations for a representative set of structures of binary FeCr alloys spanning the entire chromium concentration range between 0 and 100%. Within the Hamiltonian formalism, magnetic configurations emerge as symmetry-broken ground-state solutions. The Stoner Hamiltonian (5) is a limiting case of a general many-orbital-per-site Hamiltonian (1) and it can be derived[42] from Eq. (1) by imposing constraints stemming from the local charge-neutrality condition.

The availability of a fully parameterized many-body Stoner Hamiltonian offers a way of extending density-functional theory calculations to the case of finite temperatures *and* to the treatment of time-dependent correlated dynamics of atomic and electronic excitations. The latter may involve, for example, the use of semiclassical models where forces acting between atoms are described by effective semiempirical spin-orientation-dependent "interatomic potentials."[73]

To parameterize the Hamiltonian, we carried out two case studies. In case study I only the Stoner on-site intra-atomic exchange parameters I_i were adjusted to match the *ab initio* results. In this approximation it is already possible to reproduce the negative enthalpy-of-mixing anomaly characterizing the alloy in the low chromium concentration limit. The model parameters developed for case study II, where the hopping integrals and the Stoner parameters were derived from the electronic structure of pure Fe and pure Cr, provide a very accurate match to density-functional theory calculations. Both sets of parameters (case studies I and II) behave equally well when applied to the investigation of deformation of the most stable FeCr alloy compound along the Bain transformation pathway.

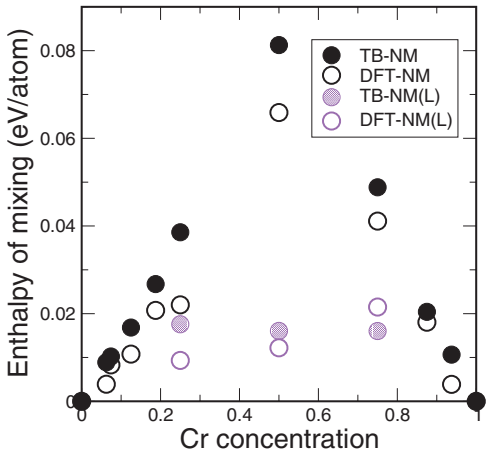

FIG. 7. (Color) The enthalpy-of-mixing for nonmagnetic bcc binary FeCr alloys calculated using the TB Hamiltonian for case study II and plotted using energies of nonmagnetic pure bcc Fe and Cr as a reference, shown together with the corresponding values found by DFT calculations.

A conclusion that follows from our study is that all the significant features characterizing FeCr alloys can be explained in terms of bonding effects involving 3*d* electron orbitals and magnetic symmetry-breaking effects resulting from intra-atomic on-site Stoner exchange. To clarify the point that the origin of anomalous negative enthalpy of mixing is associated with the presence of the Stoner on-site exchange terms in the Hamiltonian (5), in Fig. 7 we show the enthalpy of mixing for *nonmagnetic* bcc FeCr alloys calculated for case study II and plotted using energies of nonmagnetic bcc Fe and Cr as a reference. The figure also gives the corresponding DFT results. The negative enthalpies of mixing for small Cr concentrations, resulting from antiferromagnetic correlations between Cr atoms in the Fe host lattice, which in turn enhance the stability of the ferromagnetic state of diluted bcc alloys and raise the Curie temperature,[74] completely vanish in the case where there is no Stoner exchange contribution. The main contribution to the negative enthalpy-of-mixing anomaly comes from the exchange terms associated with iron sites [indeed the value of I_d(Fe) is greater than that of I_d(Cr)], taking into account the Stoner exchange on chromium sites I_d(Cr) is also important to match the magnetic DFT energies in the entire range of Cr concentrations. In the limit of high Cr concentrations, it is necessary to take into account clustering of Cr atoms (the so-called α-α' decomposition of the alloy) that occurs even at low temperatures.[5] In case study I, where bonding integrals for Fe-Fe, Cr-Cr, and FeCr sites are assumed to be identical, the nonmagnetic calculations predict very small positive values for the enthalpies of mixing for the whole range of Cr concentration. This illustrates the part played by the nonlinear magnetic terms in Eq. (5) and the fact that chemical bonds in the alloy form as a result of self-consistent evolution of electronic structure involving both intersite electron hopping and on-site exchange effects.

We also note that the positive enthalpies of mixing in Fig. 7 can be directly compared with calculations performed for a DLM FeCr system (see Fig. 3 of Ref. 10) within the coherent

potential approximations (CPA), where the reference energies correspond to paramagnetic bcc states. The DLM approximation, mimicking high-temperature magnetic configurations, can now be investigated within the present Stoner TB Hamiltonian approach following the method developed by Hasegawa *et al.*[27] for pure iron. A general treatment of orientational magnetic disorder can now also be implemented for Hamiltonian (5) following Refs. 75–77.

Therefore, the fact that we are now able to convincingly identify the type of the Hamiltonian and the specific terms responsible for the observed anomalous behavior of FeCr alloys, opens a way to deriving further approximate computational algorithms for these alloys, and steels, suitable for large-scale simulations of radiation damage effects in these materials.

ACKNOWLEDGMENTS

The authors gratefully acknowledge discussions with A. Caro, J.-L. Boutard, P. M. Derlet, M. W. Finnis, M. Y. Lavrentiev, and D. G. Pettifor. This work was supported by the UK Engineering and Physical Sciences Research Council and by EURATOM through the EFDA Fusion Materials Modeling Programme.

[1] M. Victoria, S. L. Dudarev, J.-L. Boutard, E. Diegele, R. Lässer, A. Almazouzi, M. J. Caturla, C. C. Fu, J. Källne, L. Malerba, K. Nordlund, M. Perlado, M. Rieth, M. Samaras, R. Schäublin, B. N. Singh, and F. Willaime, Fusion Eng. Des. **82**, 2413 (2007).
[2] S. L. Dudarev, J.-L. Boutard, R. Lässer, M. J. Caturla, P. M. Derlet, M. Fivel, C.-C. Fu, M. Y. Lavrentiev, L. Malerba, M. Mrovec, D. Nguyen-Manh, K. Nordlund, M. Perlado, R. Schäublin, H. Van Swygenhoven, D. Terentyev, J. Wallenius, D. Weygand, and F. Willaime, J. Nucl. Mater. **386-388**, 1 (2009).
[3] A. A. Mirzoev, M. M. Yalalov, and D. A. Mirzaev, Phys. Met. Metallogr. **97**, 336 (2004).
[4] T. P. C. Klaver, R. Drautz, and M. W. Finnis, Phys. Rev. B **74**, 094435 (2006).
[5] D. Nguyen-Manh, M. Y. Lavrentiev, and S. L. Dudarev, J. Comput.-Aided Mater. Des. **14**, 159 (2007).
[6] M. Y. Lavrentiev, R. Drautz, D. Nguyen-Manh, T. P. C. Klaver, and S. L. Dudarev, Phys. Rev. B **75**, 014208 (2007).
[7] D. Nguyen-Manh, M. Yu. Lavrentiev, and S. L. Dudarev, C. R. Phys. **9**, 379 (2008).
[8] P. Erhart, B. Sadigh, and A. Caro, Appl. Phys. Lett. **92**, 141904 (2008).
[9] P. Olsson, I. A. Abrikosov, L. Vitos, and J. Wallenius, J. Nucl. Mater. **321**, 84 (2003).
[10] P. Olsson, I. A. Abrikosov, and J. Wallenius, Phys. Rev. B **73**, 104416 (2006).
[11] A. V. Ruban, P. A. Korzhavyi, and B. Johansson, Phys. Rev. B **77**, 094436 (2008).
[12] P. A. Korzhavyi, A. V. Ruban, J. Odqvist, J. O. Nilsson, and B. Johansson, Phys. Rev. B **79**, 054202 (2009).
[13] C. Domain and C. S. Becquart, Phys. Rev. B **65**, 024103 (2001).
[14] P. Olsson, C. Domain, and J. Wallenius, Phys. Rev. B **75**, 014110 (2007).
[15] T. P. C. Klaver, P. Olsson, and M. W. Finnis, Phys. Rev. B **76**, 214110 (2007).
[16] A. T. Paxton and M. W. Finnis, Phys. Rev. B **77**, 024428 (2008).
[17] I. Mirebeau, M. Hennion, and G. Parette, Phys. Rev. Lett. **53**, 687 (1984).
[18] A. Caro, D. A. Crowson, and M. Caro, Phys. Rev. Lett. **95**, 075702 (2005).
[19] G. Liu, D. Nguyen-Manh, B.-G. Liu, and D. G. Pettifor, Phys. Rev. B **71**, 174115 (2005).
[20] D. Nguyen-Manh, V. Vitek, and A. P. Horsfield, Prog. Mater. Sci. **52**, 255 (2007).
[21] D. Nguyen-Manh, M. Mrovec, and S. P. Fitzgerald, Mater. Trans. **49**, 2497 (2008).
[22] K. Arakawa, M. Hatanaka, E. Kuramoto, K. Ono, and H. Mori, Phys. Rev. Lett. **96**, 125506 (2006); K. Arakawa, K. Ono, and H. Mori, in *Electron Microscopy and Multiscale Modelling, EMMM-2007*, edited by A. Avilov *et al.*, AIP Conf. Proc. No. CP999 (AIP, New York, 2008) pp. 66–78.
[23] S. L. Dudarev, R. Bullough, and P. M. Derlet, Phys. Rev. Lett. **100**, 135503 (2008).
[24] M. L. Jenkins, Z. Yao, M. Hernández-Mayoral, and M. A. Kirk, J. Nucl. Mater. **389**, 197 (2009).
[25] S. L. Dudarev, P. M. Derlet, and R. Bullough, J. Nucl. Mater. **386-388**, 45 (2009).
[26] S. K. Satija, R. P. Comés, and G. Shirane, Phys. Rev. B **32**, 3309 (1985).
[27] H. Hasegawa, M. W. Finnis, and D. G. Pettifor, J. Phys. F: Met. Phys. **15**, 19 (1985).
[28] S. P. Fitzgerald and S. L. Dudarev, Proc. R. Soc. London, Ser. A **464**, 2549 (2008).
[29] S. P. Fitzgerald and S. L. Dudarev, J. Nucl. Mater. **386-388**, 67 (2009).
[30] P. W. Anderson, Phys. Rev. **124**, 41 (1961).
[31] J. Friedel, J. Phys. Radium **19**, 573 (1958); Nuovo Cimento, Suppl. **7**, 287 (1958).
[32] J. Hubbard, Proc. R. Soc. London, Ser. A **276**, 238 (1963); **277**, 237 (1964); **281**, 401 (1964).
[33] J. Hubbard, Phys. Rev. B **19**, 2626 (1979); **20**, 4584 (1979).
[34] E. C. Stoner, Proc. R. Soc. London, Ser. A **169**, 339 (1939).
[35] O. Gunnarsson, J. Phys. F: Met. Phys. **6**, 587 (1976).
[36] H. Bethe and E. Salpeter, *Quantum Mechanics of One-and Two-Electron Atoms* (Academic, Berlin, 1957).
[37] S. L. Dudarev, G. A. Botton, S. Y. Savrasov, Z. Szotek, W. M. Temmerman, and A. P. Sutton, Phys. Status Solidi A **166**, 429 (1998).
[38] P. W. Anderson, in *Solid State Physics*, edited by F. Seitz and D. Turnbull (Academic, New York, 1963), Vol. 14, pp. 99–214.
[39] B. Caroli, C. Caroli, and D. R. Fredkin, Phys. Rev. **178**, 599 (1969).
[40] A. Kotani and T. Yamazaki, Prog. Theor. Phys. **108**, 117 (1992).
[41] S. L. Dudarev, G. A. Botton, S. Y. Savrasov, C. J. Humphreys, and A. P. Sutton, Phys. Rev. B **57**, 1505 (1998).
[42] S. L. Dudarev and P. M. Derlet, J. Comput.-Aided Mater. Des. **14**, 129 (2007).

[43] A. G. Khachaturyan, *Theory of Structural Transformations in Solids* (Wiley, New York, 1983).
[44] D. R. Mason, R. E. Rudd, and A. P. Sutton, J. Phys.: -Condens. Matter **16**, S2679 (2004).
[45] S. Y. Savrasov, Phys. Rev. B **54**, 16470 (1996).
[46] D. G. Pettifor, *Bonding and Structure of Molecules and Solids* (Clarendon, Oxford, 1996), pp. 180–198.
[47] J. C. Slater, *Quantum Theory of Atomic Structure* (McGraw-Hill, New York, 1960).
[48] A. M. Oles, Phys. Rev. B **28**, 327 (1983).
[49] P. Fulde, *Electron Correlations in Molecules and Solids*, 3rd ed. (Springer-Verlag, Berlin, 1995).
[50] P. Fazekas, *Electron Correlation and Magnetism* (World Scientific, Singapore, 1999).
[51] A. P. Sutton, M. W. Finnis, D. G. Pettifor, and Y. Ohta, J. Phys. C **21**, 35 (1988).
[52] W. A. Harrison, *Electronic Structure and the Properties of Solids* (W.H. Freeman, San Francisco, 1980).
[53] A. P. Horsfield, D. R. Bowler, A. M. Bratkovsky, M. Fearn, P. Goodwin, S. Goedecker, C. Goringe, D. Muller, R. Harris, and D. Nguyen-Manh, OXON code, University of Oxford, Oxford, England, 2007, http://www-mml.materials.ox.ac.uk/facilities/oxon.shtml
[54] D. Nguyen-Manh, D. G. Pettifor, and V. Vitek, Phys. Rev. Lett. **85**, 4136 (2000).
[55] D. Nguyen-Manh, T. Saha-Dasgupta, and O. K. Andersen, Bull. Mater. Sci. **26**, 27 (2003).
[56] D. Nguyen-Manh, M. Y. Lavrentiev, and S. L. Dudarev, Comput. Mater. Sci. **44**, 1 (2008).
[57] D. A. Pankhurst, D. Nguyen-Manh, and D. G. Pettifor, Phys. Rev. B **69**, 075113 (2004).
[58] P. Alvarado, J. Dorantes-Davila, and G. M. Pastor, Phys. Rev. B **58**, 12216 (1998).
[59] I. Yang, S. Y. Savrasov, and G. Kotliar, Phys. Rev. Lett. **87**, 216405 (2001).
[60] P. A. Korzhavyi, B. Sundman, M. Selleby, B. Johansson, *Integrative and Interdisciplinary Aspects of Intermetallics*, edited by Michael J. Millis *et al.*, MRS Symposia Proceedings Vol. 842 (Materials Research Society, Pittsburgh, 2005), p. S4.10.1.
[61] H. K. D. H. Bhadeshia and R. W. K. Honeycombe, *Steels: Microstructure and Properties*, 3rd ed. (Elsevier, Amsterdam, 2006).
[62] J. O. Andersson and B. Sundman, CALPHAD: Comput. Coupling Phase Diagrams Thermochem. **11**, 83 (1987).
[63] D. Nguyen-Manh and D. G. Pettifor, in *Gamma Titanium Aluminides*, edited by Y. W. Kim, D. M. Dimiduk, and M. H. Loretto (The Minerals, Metals and Materials Society, Warrendale, 1999), pp. 175–182.
[64] H. C. Herper, E. Hoffmann, and P. Entel, Phys. Rev. B **60**, 3839 (1999).
[65] Elastic constant calculations for $Fe_{15}Cr$ have been performed using Vienna *ab initio* simulation package (VASP) within the PAW GGA-PBE approximation using a cutoff energy of 400 eV and the first-order Methfessel-Paxton smearing with a width of 0.2 eV. The level of convergence of electronic iterations is 1.E-6 eV through the use of normal (blocked Davidson) algorithm and real-space projection operators.
[66] O. K. Andersen and O. Jepsen, Phys. Rev. Lett. **53**, 2571 (1984).
[67] P. M. Derlet and S. L. Dudarev, Prog. Mater. Sci. **52**, 299 (2007).
[68] V. Heine, Phys. Rev. **153**, 673 (1967).
[69] O. K. Andersen, T. Saha-Dasgupta, R. W. Tank, C. Arcangeli, O. Jepsen, and G. Krier, in *Electronic Structure and Physical Properties of Solids*, Lecture Notes in Physics Vol. 535, edited by H. Dreysse (Springer, New York, 2000).
[70] M. J. Mehl and D. A. Papaconstantopoulos, Phys. Rev. B **54**, 4519 (1996).
[71] G. J. Ackland, Phys. Rev. B **79**, 094202 (2009).
[72] *The Physics of Metals*, edited by J. M. Ziman (Cambridge University Press, New York, 1969).
[73] P.-W. Ma, C. H. Woo, and S. L. Dudarev, Phys. Rev. B **78**, 024434 (2008).
[74] M. Yu. Lavrentiev, S. L. Dudarev, and D. Nguyen-Manh, J. Nucl. Mater. **386-388**, 22 (2009).
[75] D. G. Pettifor, J. Magn. Magn. Mater. **15-18**, 847 (1980).
[76] M. van Schilfgaarde and V. P. Antropov, J. Appl. Phys. **85**, 4827 (1999).
[77] E. Martinez, R. Robles, D. Stoeffler, and A. Vega, Phys. Rev. B **74**, 184435 (2006).